

Resonant catalysis of thermally-activated chemical reactions with vibrational polaritons

Jorge A. Campos-Gonzalez-Angulo, Raphael F. Ribeiro, and Joel Yuen-Zhou*

Department of Chemistry and Biochemistry. University of California San Diego. La Jolla, California 92093, USA

In the regime of ensemble vibrational strong coupling (VSC), a macroscopic number N of molecular transitions couple to each resonant cavity mode, yielding two hybrid light-matter (polariton) modes, and a reservoir of $N - 1$ dark states whose chemical dynamics are essentially those of the bare molecules. This fact is seemingly in opposition to the recently reported modification of thermally activated ground electronic state reactions under VSC. Here, we provide a VSC Marcus-Levich-Jortner electron transfer model that potentially addresses this paradox: while entropy favors the transit through dark-state channels, the chemical kinetics can be dictated by a few polaritonic channels with smaller activation energies. The effects of catalytic VSC are maximal at light-matter resonance, in agreement with experimental observations.

Introduction

The strong interaction between excitations in a material medium and a resonant confined electromagnetic mode results in new states with light-matter hybrid character (polaritons) [1, 2]. Recent studies of molecular polaritons have revealed new phenomena and features that are appealing for applications in chemistry and materials science. These discoveries opened the doors to the emerging field of “polariton chemistry” [3–11]. Of particular interest are recent observations of chemoselective suppression and enhancement of reactive pathways for molecules whose high-frequency vibrational modes are strongly coupled to infrared optical cavities [12–15]. These effects of vibrational strong coupling (VSC) are noteworthy in that they occur in the absence of external photon pumping; implying that they involve thermally-activated (TA) processes, and potentially paving the road for a radically new synthetic chemistry strategy that involves injecting microfluidic solutions in suitable optical cavities to induce desired transformations. It is important to highlight that the VSC in these samples is the consequence of an ensemble effect: each cavity mode (that is resonant with the polarization of the material) coherently couples to a large number of molecules. This coupling leads to two polaritonic modes and a macroscopic set of quasi-degenerate dark (subradiant) modes that, to a good approximation, should feature chemical dynamics that is indistinguishable from that of the bare molecular modes [16]. This picture could potentially change as a consequence of ultrastrong coupling effects; however, these effects should not be significant for modest Rabi splittings as those observed in the experiments [12–15].

From the population of vibrationally excited states at thermal equilibrium, a tiny fraction would be allocated to the polariton modes, with the overwhelming majority residing in the dark-state reservoir [17–20], unless the temperature is low enough for the lower polariton to overtake the predominant population second to that of the ground

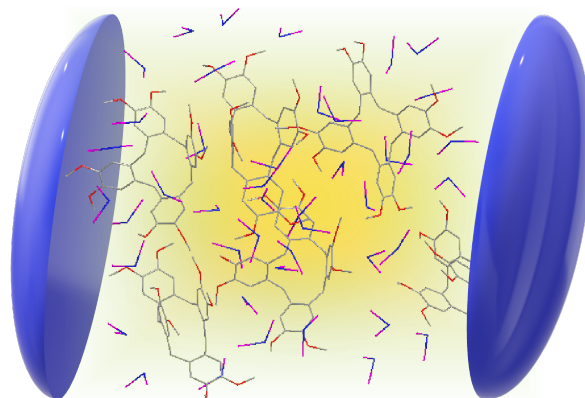


FIG. 1. Depiction of a microcavity encasing a large number of molecules that can undergo a chemical reaction (e.g., electron-transfer induced conformational transformation[24]) and support a high-frequency vibrational mode that can strongly couple to a confined optical mode; these molecules are in a solvated environment (blue/purple moieties). The reaction of concern is mediated by that intramolecular mode and a low-frequency collective configuration of the solvation sphere.

state. It is thus puzzling and remarkable that differences in the chemical kinetics can be detected in macroscopic systems under VSC at room temperature. This article provides a possible rationale for these observations. By studying a VSC version of the well-established Marcus-Levich-Jortner (MLJ) TA electron transfer model [21–23], we find a parameter range where, even if the number of dark-state channels massively outweigh the few polaritonic ones, the latter dictate the kinetics of the reaction given their smaller activation energies. The present model does not feature the complexity of the experimentally studied systems; however, it provides a minimalistic conceptual framework to develop qualitative insights on general TA VSC processes. We believe that this mechanism of polaritonic activation barrier reduction might be a widespread feature among such processes.

* joelyuen@ucsd.edu

Results

Theoretical framework

According to MLJ theory, the rate coefficient of charge-transfer from a reactant (R) to a product (P) electronic state, at constant temperature T , is given by [21–23]

$$k_{R \rightarrow P} = \sqrt{\frac{\pi}{\lambda_S k_B T}} \frac{|J_{RP}|^2}{\hbar} e^{-S} \times \sum_{v=0}^{\infty} \frac{S^v}{v!} \exp\left(-\frac{(\Delta E + \lambda_S + v\hbar\omega_P)^2}{4\lambda_S k_B T}\right), \quad (1)$$

where J_{RP} is the non-adiabatic coupling between electronic states, λ_S is the outer-sphere reorganization energy related to the low-frequency (classical) degrees of freedom of the solvent, ω_P is the frequency of a high-frequency intramolecular (quantum) mode with quantum number labeled by v , $S = \lambda_P/\hbar\omega_P$ is a Huang-Rhys parameter with λ_P the reorganization energy of the quantum mode, ΔE is the difference in energy between the equilibrium configurations of the R and P potential energy surfaces, and k_B is the Boltzmann constant. The MLJ rate can be thought of as a generalization of Marcus theory to include a sum over channels with different quanta v in the high-frequency mode of the product.

To gauge the effects of VSC, we consider the interaction between a single microcavity mode and an ensemble of M molecules that undergo electron transfer. For simplicity, we assume that VSC occurs via the high-frequency mode of P (since the MLJ rate only accounts for transitions originated in the ground state of the reactants, the case where this coupling also happens through R shares features with the current one that we shall discuss later). This constraint implies a drastic change in molecular geometry upon charge transfer so that the vibrational transition dipole moment goes from negligible to perceptible. This rather unusual behavior can be observed in molecular actuators.[24, 25] The Hamiltonian for such system is

$$\hat{H} = \hat{H}_{\text{ph}} + \sum_{i=1}^M \left[\hat{H}_R^{(i)} |R_i\rangle\langle R_i| + \left(\hat{H}_P^{(i)} + \hat{V}_{\text{int}}^{(i)} \right) |P_i\rangle\langle P_i| + J_{RP} (|R_i\rangle\langle P_i| + |P_i\rangle\langle R_i|) \right], \quad (2)$$

where $\hat{H}_{\text{ph}} = \hbar\omega_0 \left(\hat{a}_0^\dagger \hat{a}_0 + \frac{1}{2} \right)$ is the Hamiltonian of the electromagnetic mode with frequency ω_0 , $|R_i\rangle$ and $|P_i\rangle$ denote the electronic (reactant/product) states of the i -th molecule, $\hat{H}_R^{(i)} = \hbar\omega_R \hat{\mathcal{D}}_i^\dagger \hat{\mathcal{S}}_i^\dagger \left(\hat{a}_i^\dagger \hat{a}_i + \frac{1}{2} \right) \hat{\mathcal{S}}_i \hat{\mathcal{D}}_i + \hat{H}_S(\hat{\mathbf{q}}_S^{(i)} + \mathbf{d}_S)$ and $\hat{H}_P^{(i)} = \hbar\omega_P \left(\hat{a}_i^\dagger \hat{a}_i + \frac{1}{2} \right) + \hat{H}_S(\hat{\mathbf{q}}_S^{(i)}) + \Delta E$ are the bare Hamiltonians of the i -th reactant/product with quantum mode frequency ω_R and ω_P , respectively. $\hat{V}_{\text{int}}^{(i)} = \hbar g \left(\hat{a}_i^\dagger \hat{a}_0 + \hat{a}_0^\dagger \hat{a}_i \right)$ is the light-matter interaction under the rotating wave approximation [26] with single-molecule coupling $g = -\mu \sqrt{\frac{\hbar\omega_0}{2V\varepsilon_0}}$,

transition dipole moment μ , and cavity mode volume V , $\hat{a}_i^\dagger/\hat{a}_i$ are creation/annihilation operators acting on the quantum mode of the i -th molecule ($i = 0$ denotes the cavity mode), $\hat{\mathcal{S}}_i = \exp\left[\frac{1}{2} \ln\left(\sqrt{\frac{\omega_P}{\omega_R}}\right) (\hat{a}_i^{\dagger 2} - \hat{a}_i^2)\right]$ and $\hat{\mathcal{D}}_i = \exp\left[\frac{1}{\sqrt{2}} (\hat{a}_i^\dagger - \hat{a}_i) d_P\right]$ are squeezing and displacement operators [26] (see §S1 for the origin of these terms), $\hat{H}_S(\hat{\mathbf{q}}_S^{(i)}) = \sum_\ell \frac{1}{2} \hbar \omega_S^{(\ell)} \left(\hat{p}_S^{(i,\ell)2} + \hat{q}_S^{(i,\ell)2} \right)$ is the Hamiltonian of the classical modes with frequencies $\omega_S^{(\ell)}$, $\hat{\mathbf{p}}_S^{(i)}$ and $\hat{\mathbf{q}}_S^{(i)}$ are the set of rescaled classical momenta and positions associated with the i -th quantum mode, and d_P and \mathbf{d}_S are the rescaled (dimensionless) distances between equilibrium configurations of the reactant and product along the quantum and classical mode coordinates, respectively. We shall point out that, since it only considers coupling to a single cavity mode, the Hamiltonian in Eq. (2) entails coarse-graining; therefore, M is not the total number of molecules in the cavity volume, but the average number of molecules coupled per cavity mode [17]. While polaritonic effects in electron transfer processes have been studied in the pioneering work of [27] (see also [28]), we note that they were considered in the *electronic* strong coupling regime; as we shall see, the vibrational counterpart demands a different formalism and offers conceptually different phenomenology.

As a consequence of VSC, the system is best described in terms of collective normal modes defined by the operators [7, 29]

$$\begin{aligned} \hat{a}_{+(N)} &= \cos\theta_N \hat{a}_0 - \sin\theta_N \hat{a}_{B(N)}, \\ \hat{a}_{-(N)} &= \sin\theta_N \hat{a}_0 + \cos\theta_N \hat{a}_{B(N)}, \\ \hat{a}_{D(N)}^{(k)} &= \sum_{i=1}^N c_{ki} \hat{a}_i; \quad 2 \leq k \leq N \end{aligned} \quad (3)$$

where $0 \leq N \leq M$ is the number of molecules in the P state at a given stage in the reaction. These operators correspond to the upper and lower polaritons (UP , LP), and dark (D) modes, respectively. Note that the operators $\hat{a}_{D(N)}^{(k)}$ are defined only for $N \geq 2$, and the coefficients c_{ki} fulfill $\sum_{i=1}^N c_{ki} = 0$ and $\sum_{i=1}^N c_{k'i}^* c_{ki} = \delta_{k'k}$. In Eq. (3), $\theta_N = \frac{1}{2} \arctan \frac{2g\sqrt{N}}{\Delta}$ is the mixing angle, where $\Delta = \omega_0 - \omega_P$ is the light-matter detuning, and $\hat{a}_{B(N)} = \frac{1}{\sqrt{N}} \sum_{i=1}^N \hat{a}_i$ corresponds to the so-called bright (superradiant) mode. These modes have associated frequencies

$$\begin{aligned} \omega_{\pm(N)} &= \frac{\omega_0 + \omega_P}{2} \pm \frac{\Omega_N}{2}, \\ \omega_D &= \omega_P, \end{aligned} \quad (4)$$

where $\Omega_N = \sqrt{4g^2 N + \Delta^2}$ is the effective Rabi splitting; equivalent definitions can be made for the creation operators. Note that there is no “free-lunch”: the super-radiantly enhanced VSC with the bright mode occurs at the expense of the creation of a macroscopic number of

dark modes that –under the context of this model– do not mix with light. (Inhomogeneous broadening results in small but experimentally observable light-like character for these modes [29–32]. This effect is negligible for the phenomena considered in this work given that the density of molecular excitations is much larger than that of the photon modes.)

Inside of the cavity, the reaction $R \rightarrow P$ becomes

$$R + UP_{N-1} + LP_{N-1} + \sum_{k=2}^{N-1} D_{N-1}^{(k)} \rightarrow UP_N + LP_N + \sum_{k=2}^N D_N^{(k)}, \quad (5)$$

where the subscripts indicate the number of molecules that participate in VSC (from Eq. (3) it can be seen that UP_0 corresponds to the uncoupled photon mode, and LP_0 and $D_0^{(k)}$ are nonexistent). This reaction implies that each time a molecule transforms into the product, it becomes part of the ensemble that couples to light (see §S2 for additional insight). Electron transfer occurs as a result of a vibronic transition between diabatic states; this feature makes it similar to Raman scattering. A study of the latter under VSC [33] took advantage of the massive degeneracy of the dark modes to introduce a judicious basis [34],

$$\hat{a}_D^{(k)} = \frac{1}{\sqrt{k(k-1)}} \left(\sum_{i=1}^{k-1} \hat{a}_i - (k-1)\hat{a}_k \right), \quad (6)$$

that enables calculations for an arbitrary number of

molecules, and will prove to be convenient for our purposes. Notice that the mode $\hat{a}_D^{(k)}$ is highly localized at \hat{a}_k but has a long tail for $\hat{a}_{1 \leq i \leq k-1}$ (for a visualization, see Fig. S1); furthermore, it is fully characterized by the index k , and thus does not depend explicitly on N . In terms of these dark modes, the reaction in Eq. (5) can be drastically simplified from an $N+1$ to a three-body process,

$$R + UP_{N-1} + LP_{N-1} \rightarrow UP_N + LP_N + D_N^{(N)}, \quad (7)$$

where, without loss of generality, we have considered that the N -th molecule is the one that undergoes the reaction (notice that, in accordance with the notation introduced in Eq. (6), the mode $D_N^{(N)}$ is highly localized in P_N for sufficiently large N). Furthermore, we can identify the normal modes of the photon (\hat{a}_0), the N -th molecule (\hat{a}_N), and the bright state that excludes it ($\hat{a}_{B(N-1)}$) as natural degrees of freedom of the problem since the modes in reactants and products can be written as Duschinsky transformations [35] of these. Explicitly, for the reactants we have

$$\begin{pmatrix} \hat{a}_{+(N-1)} \\ \hat{a}_{-(N-1)} \end{pmatrix} = \begin{pmatrix} \cos \theta_{N-1} & -\sin \theta_{N-1} \\ \sin \theta_{N-1} & \cos \theta_{N-1} \end{pmatrix} \begin{pmatrix} \hat{a}_0 \\ \hat{a}_{B(N-1)} \end{pmatrix}, \quad (8)$$

$$\hat{a}'_N = \hat{\mathcal{D}}_N^\dagger \hat{\mathcal{S}}_N^\dagger \hat{a}_N \hat{\mathcal{S}}_N \hat{\mathcal{D}}_N, \quad (9)$$

where \hat{a}'_N acts on the vibrational degrees of freedom of the N -th reactant (see §S1 for a derivation); while for the products

$$\begin{pmatrix} \hat{a}_{+(N)} \\ \hat{a}_{-(N)} \\ \hat{a}_D^{(N)} \end{pmatrix} = \begin{pmatrix} \cos \theta_N & -\sin \theta_N & 0 \\ \sin \theta_N & \cos \theta_N & 0 \\ 0 & 0 & 1 \end{pmatrix} \begin{pmatrix} 1 & 0 \\ 0 & \sqrt{\frac{N-1}{N}} & \sqrt{\frac{1}{N}} \\ 0 & \sqrt{\frac{1}{N}} & -\sqrt{\frac{N-1}{N}} \end{pmatrix} \begin{pmatrix} \hat{a}_0 \\ \hat{a}_{B(N-1)} \\ \hat{a}_N \end{pmatrix}. \quad (10)$$

With the above considerations, the VSC analogue of the MLJ rate coefficient in Eq. (1) is given by a sum over possible quanta $\{v_+, v_-, v_D\}$ in the product modes UP_N , LP_N and $D_N^{(N)}$, respectively:

$$k_{R \rightarrow P}^{VSC} = \sqrt{\frac{\pi}{\lambda_S k_B T}} \frac{|J_{RP}|^2}{\hbar} \sum_{v_+=0}^{\infty} \sum_{v_-=0}^{\infty} \sum_{v_D=0}^{\infty} W_{v_+, v_-, v_D}, \quad (11)$$

where $W_{v_+, v_-, v_D} = |F_{v_+, v_-, v_D}|^2 \exp\left(-\frac{E_{v_+, v_-, v_D}^\ddagger}{k_B T}\right)$, and

$$\begin{aligned} |F_{v_+, v_-, v_D}|^2 &= |\langle 0_{+(N-1)} 0_{-(N-1)} 0_R | v_+ v_- v_D \rangle|^2 \\ &= \left(\frac{\sin^2 \theta_N}{N}\right)^{v_+} \left(\frac{\cos^2 \theta_N}{N}\right)^{v_-} \left(\frac{N-1}{N}\right)^{v_D} \\ &\quad \times \left(\frac{v_+ + v_- + v_D}{v_+, v_-, v_D}\right) |\langle 0' | v_+ + v_- + v_D \rangle|^2, \end{aligned} \quad (12)$$

is a Franck-Condon factor between the global ground state in the reactants and the excited vibrational configuration in the product [33]. Here, $|0'\rangle$ is the vibrational ground state of the N -th molecule in the reactant electronic state and $|v_+ + v_- + v_D\rangle$ is the vibrational state of the N -th molecule with $v_+ + v_- + v_D$ in the product

electronic state. The calculation in Eq. (12) (see §S3 for a derivation) is reminiscent to the contemporary problem of boson sampling [36]. Using the notation from Eq. (1),

$$E_{v_+,v_-,v_D}^\ddagger = \frac{(E_P^{v_+,v_-,v_D} - E_R^0 + \lambda_S)^2}{4\lambda_S}, \quad (13)$$

is the activation energy of the channel, with $E_R^0 = \frac{\hbar}{2}(\omega_{+(N-1)} + \omega_{-(N-1)} + \omega_R)$ and $E_P^{v_+,v_-,v_D} = \Delta E + \hbar[\omega_{+(N)}(v_+ + \frac{1}{2}) + \omega_{-(N)}(v_- + \frac{1}{2}) + \omega_P(v_D + \frac{1}{2})]$. Eq. (12) affords a transparent physical interpretation: the state $|v_+v_-v_D\rangle$ is accessed by creating $v_+ + v_- + v_D$ excitations in the high-frequency oscillator of the N -th product; there are $\binom{v_++v_-+v_D}{v_+,v_-,v_D}$ ways to do so; $\left(\frac{\sin^2\theta_N}{N}\right)$, $\left(\frac{\cos^2\theta_N}{N}\right)$, and $\left(\frac{N-1}{N}\right)$ are the projections of the product normal modes on the oscillator of the N -th product; these scalings are the same as those obtained in our studies on polariton assisted energy transfer (PARET) [37].

Conditions for rate enhancement

When $\omega_R = \omega_P$ and $N \gg 1$, the expressions for the Franck-Condon factor and activation energy simplify to

$$|F_{v_+,v_-,v_D}|^2 = \frac{e^{-S}}{v_+!v_-!v_D!} \left(\frac{S\sin^2\theta}{N}\right)^{v_+} \left(\frac{S\cos^2\theta}{N}\right)^{v_-} S^{v_D}, \quad (14)$$

$$E_{v_+,v_-,v_D}^\ddagger = \frac{[\Delta E + \lambda_S + \hbar(v_+\omega_+ + v_-\omega_- + v_D\omega_P)]^2}{4\lambda_S}, \quad (15)$$

where we have dropped the dependence of angles and frequencies on N for brevity. For most of the experiments that have achieved VSC [12, 16, 19, 38–41], the number of molecules that take part in the coupling is between $N = 10^6$ and 10^{10} per cavity mode [17]. For such orders of magnitude, at first glance, Eq. (12) would suggest that the contribution from the dark modes dominates the rate, which, according to Eq. (14), is the same as the bare case (Eq. (1)) for $v_D = 1$ and $v_+ = v_- = 0$, i.e., if the polaritons are not employed in the reaction. In fact, this was the conclusion for PARET [37], where coupling the product to transitions to the cavity led to no change in energy transfer from reactant molecules. However, the TA processes in electron transfer kinetics offers a new dimension to the problem that PARET does not feature. Careful inspection of the expressions at hand hints to the existence of parameters ΔE and λ_S for which changes in the activation energy for the polariton channels dominate the rate. To find those parameters, we need first that the contribution going to the first vibrational excitation outplay that between ground states, i.e., $W_{001} > W_{000}$, which implies

$$\frac{\lambda_P}{\hbar\omega_P} > \exp\left(\frac{\hbar\omega_P}{4\lambda_S k_B T} [2(\Delta E + \lambda_S) + \hbar\omega_P]\right). \quad (16)$$

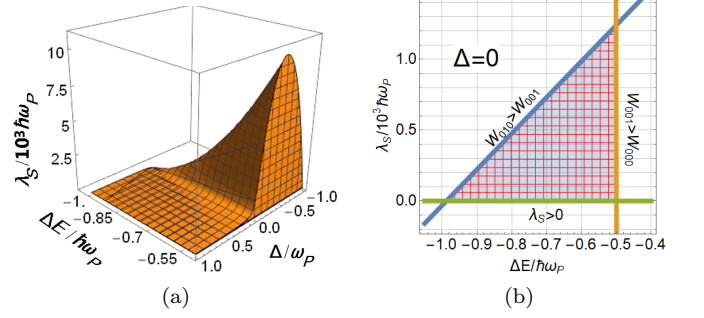


FIG. 2. Region of parameters for which the lower polariton (LP) channel dominates the kinetics over the many dark (D) channels. ΔE is the energy difference between product P and reactant R , λ_S is the classical reorganization energy, and Δ is the detuning between the cavity and the high-frequency mode of the product. In (a) we explore the three variables, while in (b) we show the cross section under resonant conditions. For these calculations, the high frequency modes are equal $\omega_R = \omega_P$, $k_B T = 0.2\hbar\omega_P$, $N = 10^{10}$, $S = 1$, and the Rabi splitting is $\hbar\Omega = 5 \times 10^{-2}\hbar\omega_P$.

Next, if the contribution from the channel where the product is formed with an excitation in the LP mode ($v_- = 1$, and $v_+ = v_D = 0$) dominates, then $W_{010} > W_{001}$, which yields

$$\frac{N}{\cos^2\theta} < \exp\left(\frac{\hbar(\Omega_N - \Delta)}{4\lambda_S k_B T} \times \left[\Delta E + \lambda_S + \hbar\omega_P + \frac{\hbar(\Delta - \Omega_N)}{4}\right]\right). \quad (17)$$

The region of parameters that satisfies these inequalities for room-temperature ($k_B T \approx 0.2\hbar\omega_P$) and typical experimental VSC Rabi-splittings $\hbar\Omega$ ($\approx 0.1\hbar\omega_P$) [12, 40] is illustrated in Fig. 2a. The order of magnitude of the plotted ΔE values is reasonably standard for this kind of processes [42, 43], which suggests the experimental feasibility of attaining these conditions.

The effect of the electromagnetic mode and the conditions for which the enhancement of the polaritonic coupling can be achieved is illustrated in Figure 3. We can understand this effect as follows; the reaction takes place as a multi-channel process consisting of an electronic transition from the reactant global ground state into the product electronic state dressed with high-frequency vibrational excitations. As shown in Figs. 3 and S2, the channel between global ground states is in the Marcus inverted regime [44, 45] and, given the small value of the classical reorganization energy, the activation energy is fairly high. On the other hand, the channel to the first excited manifold is in the normal regime with a much lower activation energy, but the range of parameters implies that the decrease in activation energy for the channel with an excitation in the LP mode is enough to overcome the elevated multiplicity of the dark modes (Figs. 3 and S2), and effectively catalyze the electron transfer

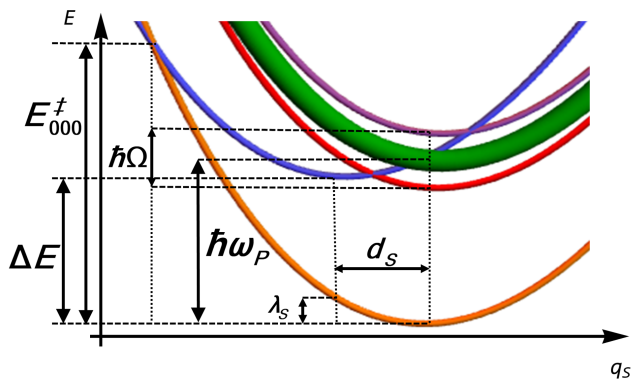


FIG. 3. Potential energy surfaces of the electronic states under VSC as a function of the slow coordinate q_s (not to scale). With respect to the reactant (blue), the vibrational ground state of the product (orange) is in the Marcus inverted regime; the manifold of states with one vibrational excitation (green, red and purple) in the product is in the normal regime. While the dark states (green) outnumber the lower (red) and upper (purple) polaritons, the small activation energy associated with the lower polariton channel might make it the preferred pathway for reactivity.

process. In terms of the expression for the rate coefficient, even though the entropic pre-exponential factor of the D channel is $N-1$ larger than that of the LP channel, the latter is associated with a larger exponential factor (lower activation energy).

In Fig. 2a we also show the parameter space that produces polaritonic enhancement as a function the detuning Δ . It can be noticed that the range of admissible values for the classical reorganization energy increases as the detuning becomes negative. This can be understood from the fact that, for negative detunings, the frequency of the photon is smaller than that of the vibrational high-frequency mode and, therefore, the activation energy to LP is lower than that corresponding to D , thus providing more flexibility for parameters to fulfill the inequalities in Eq. (17). However, we must remark that this effect disappears at sufficiently large detunings, as the matter character of the LP becomes negligible to effectively mediate the electron transfer.

Simulation of modified kinetics

The overall effect of the cavity in the charge transfer kinetics is displayed in Fig. 4, where we show the ratio of the rate coefficients, calculated inside ($k_{R \rightarrow P}$) and outside ($k_{R \rightarrow P}^{VSC}$) of the cavity as a function of the collective coupling $g\sqrt{N}/\omega_P$, for several values of detuning. The bell-shaped curves reflect the fact that, as the Rabi splitting increases, the activation energy of the LP decreases, thus making this channel the most prominent one. This trend goes on until $E_{010}^\ddagger = 0$, where this LP channel goes from the normal Marcus regime to the inverted one, and the activation energy starts to increase with the coupling until this pathway is rendered insignificant as compared to the transition to the D manifold, giving rise to kinetics

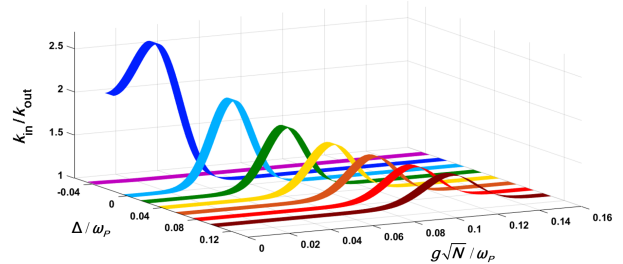


FIG. 4. Ratio between the rate coefficient inside the cavity, $k_{\text{in}} = k_{R \rightarrow P}^{VSC}$ with respect to the rate constant outside of the cavity $k_{\text{out}} = k_{R \rightarrow P}$ at several detunings Δ . For these calculations $1 \leq N \leq 10^{11}$, $\omega_R = \omega_P$, $k_B T = 0.2\hbar\omega_P$, $S = 1$, $\hbar g = 1.6 \times 10^{-5}\hbar\omega_P$ and $E_{001}^\ddagger = 4.9\hbar\omega_P$. In agreement with Marcus theory, as the lower polariton channel lowers in energy (with increasing Rabi splitting), its corresponding activation energy falls and then rises, thus dominating the kinetics and becoming irrelevant, respectively. Notice that the trend of apparent enhancement at negative detunings eventually stops at low values of $|\Delta|$.

indistinguishable from the bare molecules. The observation that larger detunings require stronger coupling to reach the maximum ratio of rate coefficients is consistent with the fact that $\hbar\Omega$ increases sublinearly with $\hbar g\sqrt{N}$; therefore, larger detunings require larger couplings to attain the same splitting. Additionally, the trend observed in the maxima, which decrease with the detuning, can be regarded as a consequence of the previous effect: the larger couplings required to reach the zero-energy-barrier are achieved with more of molecules; thus, the contribution of LP becomes less relevant than that of D , as can be seen from the pre-exponential factors. Finally, a peculiar result is the fact that the effect on the rate coefficient is more prominent in a range of few molecules for slightly negative detunings. This observation should not come as surprising since, as previously mentioned, under this condition, the LP mode has a substantially decreased activation energy; therefore, for as small as it is, the light-matter coupling is enough to open a very favored channel that accelerates the reaction. This effect might end up quenched by dissipation; however, even in the absence of the latter, it becomes irrelevant for the cumulative kinetics, as we shall see next.

Up until now, we have shown that the rate coefficient depends on the number of molecules that take part in the VSC, which changes as the reaction progresses. To illustrate the cumulative effect on the kinetics, we numerically integrate the rate law

$$\frac{d\langle N_R \rangle}{dt} = -\langle k_{R \rightarrow P}^{VSC}(N_R)N_R \rangle \quad (18)$$

where $\langle \cdot \rangle$ indicates an average over the ensemble of reactive trajectories (see §S4). We show the behavior of $N_R(t) = M - N(t)$ for several detunings in Fig. 5. In writing Eq. (18) we have assumed that every electron transfer event is accompanied by a much faster thermal-

ization of the products (largely into the global ground state in the products side) that allows us to ignore back-reactions. This assumption is well justified if we consider that, for systems with parameters close to our model molecule, the vibrational absorption linewidth is of the order of $0.01\hbar\omega_P$ [12, 19, 40], which represents a timescale suitably shorter than the reaction times estimated from the rate constant, $k_{R\rightarrow P} = 9.4 \times 10^{-6}\omega_P$, calculated with the same parameters. In Fig. 5 we can see that, for $\Delta \geq 0$, at early times the reactions proceed in the same way as in the bare case. However, after some molecules have been gathered in the product, the coupling is strong enough for the LP channel to open and dominate over the D ones. This effect is cumulative, and the reaction endures a steady catalytic boost. Importantly, the maximum enhancement is observed for resonant conditions where the light-matter coupling is the most intense. On the other hand, with a slightly negative detuning, $\Delta = -0.02\omega_P$, the reaction is intensified in the early stages (as explained above) but is taken over by the dark states after a relatively short amount of time. Although this off-resonant effect might look appealing, it occurs at an early stage of the reaction when VSC is not technically operative, namely, when the energetic separation between dark and polaritonic modes might be blurred by dissipative processes. These considerations are beyond the scope of the current article and will be systematically explored in future work. In conclusion, even though some off-resonant effects might be present at the rate coefficient level, the condition of resonance is essential to observe a significant cumulative acceleration of the reaction (i.e., change in reactant lifetime) with respect to the bare case.

Importantly, in the case where the high-frequency mode of the reactant molecules also couples to light, the system is under VSC before the reaction begins and the spectrum in the first excited manifold in the products remains invariant throughout the reaction. Therefore, the rate coefficient is a true rate constant evaluated at $N = M$, i.e., at the maximum coupling. We will present a detailed analysis of this problem elsewhere.

Discussion

We have shown that VSC can result in catalysis of TA reactions. We have presented an MLJ model to study charge transfer processes under VSC (in passing, these results suggest a VSC alternative to enhance charge conduction which has so far been only considered in the electronic strong coupling regime [37, 46–49]). In this model, there is a range of molecular features where the shrinkage of the activation energy of the lower polariton channel can outcompete the rate associated with the massive number of dark-state channels. This model describes a mechanism suitable to be present in a wide variety of thermally activated nonadiabatic reactions, e.g., electron, proton and methyl transfer, among others. We have found a range of molecular parameters where the shrinkage of the activation energy of the lower polar-

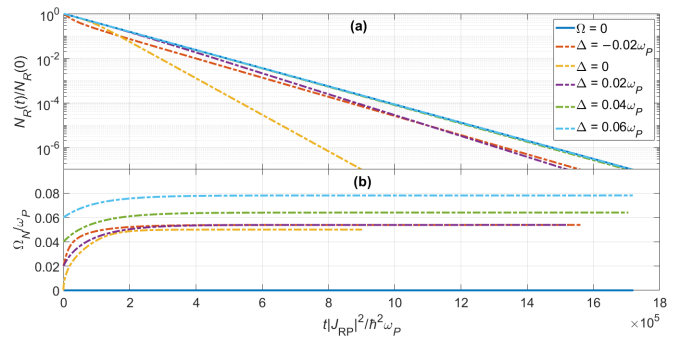


FIG. 5. a) Integrated rate law for the reaction outside and inside of the cavity at several detunings. The departure of the VSC enhanced kinetics with respect to the bare case becomes more significant at resonance. b) Evolution of effective Rabi splittings as the reaction progresses. The effects on the kinetics are observed when the VSC regime ($\Omega_N > 0.01\omega_P$) is achieved. For these calculations $M = N_R(0) = 10^7$, $\omega_R = \omega_P$, $k_B T = 0.2\hbar\omega_P$, and $E_{001}^\ddagger = 3.5\hbar\omega_P$.

ton channel can outcompete the rate associated with the massive number of dark-state channels. We determined that these effects are most prominent under resonant conditions. This finding is relevant since such is the behavior observed in experimentally in reactions performed under VSC. We must remark, however, that these are vibrationally adiabatic reactions and the involvement of the present mechanism is not obvious (for a recent study on possibly important off-resonant Casimir-Polder effects, we refer the reader to [50]). While a thorough understanding of the reaction pathways involved in these observations is beyond the scope of this article, we believe that the tug-of-war between the activation energy reduction from few polariton channels against the numerical advantage of the dark states could be a ubiquitous mechanism of TA polariton chemistry under VSC, independently of whether it occurs with reactants or products. Even though there might be other subtle physical mechanisms underlying VSC TA reactions, we conclude with three important observations regarding the presently proposed catalytic mechanism. First, it does not offer a reduction of reaction rate coefficients; after all, if the polariton channels do not provide incentives for their utilization, the dark states will still be accessible, leading to virtually unaffected reaction rates as compared with the bare case. However, an experimental suppression of reactions by VSC under TA conditions (as in [12, 13]) could correspond, microscopically, to the polaritonic modification of elementary step rates in the network of reaction pathways that comprises the mechanism. Second, it is not evident whether the conclusions associated with this mechanism are relevant in photochemical processes where nonequilibrium initialization of polariton populations is allowed. Finally, it is important to emphasize that this VSC mechanism is not guaranteed to yield changes in TA reactivity, given that particular geometric molecular conditions need to be fulfilled. Regardless, it is remarkable

that TA reactions under VSC can be modified at all given the entropic limitations imposed by the dark states. It is of much interest to the chemistry community to unravel the broader class of reactions and the VSC conditions for which this mechanism is operative; this will be part of our future work.

Methods

To calculate the consumption of the reactant as the polaritonic ensemble grows, we performed a finite-difference numerical integration of Eq. (18). Since the rate coefficient remains constant during a single molecule event, we assume a mean-field ansatz

$$\begin{aligned} \langle k_{R \rightarrow P}^{VSC}(N_R)N_R \rangle(t) &\simeq k_{R \rightarrow P}^{VSC}(\langle N_R \rangle(t))\langle N_R \rangle(t), \\ \langle k_{R \rightarrow P}^{VSC}(N_R)N_R \rangle(t + \Delta t) &\simeq k_{R \rightarrow P}^{VSC}(\langle N_R \rangle(t))(\langle N_R \rangle(t) - 1), \end{aligned} \quad (19)$$

which enables the stepwise integration of Eq. (18) with limits $t \rightarrow t + \Delta t$ and $N_R \rightarrow N_R - 1$, yielding

$$\Delta t(N_R) = \frac{1}{k_{R \rightarrow P}^{VSC}(N_R)} \ln \frac{N_R}{N_R - 1}. \quad (20)$$

We verified that this mean-field method gives numerically consistent results with the stochastic simulation algorithm (see §S4) [51], in agreement with recent studies of mean-field solutions to polariton problems in the ensemble regime [52]. The rate coefficient $k_{R \rightarrow P}^{VSC}(N_R)$ at each step is calculated from Eq. (11) truncating the sum up to $v_+ = v_- = v_D = 2$; terms beyond these excitations do not contribute appreciably given their huge activation energies resulting from the chosen parameters. The Franck-Condon and exponential factors are calculated respectively from Eq. (12) and Eq. (13) by setting $\omega_R = \omega_P$.

Acknowledgments

J.A.C.G.A thanks Matthew Du and Luis Martnez-Martnez for useful discussions. J.A.C.G.A. acknowledges initial support of the UC-MEXUS-CONACYT graduate scholarship ref. 235273/472318. J.A.C.G.A and R.F.R. were sponsored by the AFOSR award FA9550-18-1-0289. J.Y.Z. was funded with the NSF EAGER Award CHE 1836599. All the authors thank Blake Simpkins at NRL and Jonathan Keeling at University of St. Andrews for their insightful comments about the manuscript.

Author contributions

J.A.C.G.A. carried out the theoretical setup of the electron transfer reaction in terms of polariton and dark modes. J.A.C.G.A. and R.F.R. calculated the Franck-Condon factors and developed the Marcus-Levich-Jortner model. J.Y.Z. provided guidance on the interpretation of the results. All the authors contributed equally to the manuscript.

Competing interests

The authors declare no competing interests.

Data availability statement

Data sharing not applicable to this article as no datasets were generated or analysed during the current study.

Code availability statement

The source code for the simulation of the modified kinetics is available from the corresponding author upon request.

References

- [1] Hopfield, J. J. Theory of the contribution of excitons to the complex dielectric constant of crystals. *Phys Rev* **112**, 1555–1567 (1958).
- [2] Agranovich, V. M. & Malshukov, A. G. Surface polariton spectra if the resonance with the transition layer vibrations exist. *Opt Commun* **11**, 169–171 (1974).
- [3] Ebbesen, T. W. Hybrid Light-Matter States in a Molecular and Material Science Perspective. *Acc Chem Res* **49**, 2403–2412 (2016).
- [4] Bennett, K., Kowalewski, M. & Mukamel, S. Novel photochemistry of molecular polaritons in optical cavities. *Faraday Discuss* **194**, 259–282 (2016).
- [5] Sukharev, M. & Nitzan, A. Optics of exciton-plasmon nanomaterials. *J Phys : Condens Matter* **29**, 443003 (2017).
- [6] Baranov, D. G., Wersäll, M., Cuadra, J., Antosiewicz, T. J. & Shegai, T. Novel nanostructures and materials for strong light-matter interactions. *ACS Photonics* **5**, 24–42 (2018).
- [7] Ribeiro, R. F., Martínez-Martínez, L. A., Du, M., Campos-Gonzalez-Angulo, J. & Yuen-Zhou, J. Polariton chemistry: controlling molecular dynamics with optical cavities. *Chem Sci* **9**, 6325–6339 (2018).
- [8] Flick, J., Rivera, N. & Narang, P. Strong light-matter coupling in quantum chemistry and quantum photonics. *Nanophotonics* **7**, 1479 (2018).
- [9] Stranius, K., Hertzog, M. & Börjesson, K. Selective manipulation of electronically excited states through strong light-matter interactions. *Nature Communications* **9**, 2273 (2018).
- [10] Ruggenthaler, M., Tancogne-Dejean, N., Flick, J., Appel, H. & Rubio, A. From a quantum-electrodynamical light-matter description to novel spectroscopies. *Nature Reviews Chemistry* **2**, 0118 (2018).
- [11] Feist, J., Galego, J. & Garcia-Vidal, F. J. Polaritonic chemistry with organic molecules. *ACS Photonics* **5**, 205–216 (2018).
- [12] Thomas, A. *et al.* Ground-state chemical reactivity under vibrational coupling to the vacuum electromagnetic field. *Angew Chem Int Ed* **55**, 11462–11466 (2016).
- [13] Thomas, A. *et al.* Tilting a ground-state reactivity landscape by vibrational strong coupling. *Science* **363**, 615 (2019).
- [14] Hiura, H., Shalabney, A. & George, J. Cavity catalysis – accelerating reactions under vibrational strong coupling– (2018). Preprint, posted April 11, 2018.
- [15] Lather, J., Bhatt, P., Thomas, A., Ebbesen, T. W. & George, J. Cavity catalysis by cooperative vibrational strong coupling of reactant and solvent molecules. *Angewandte Chemie International Edition* **58**, 10635–10638 (2019).

- [16] Dunkelberger, A. D., Davidson, R. B., Ahn, W., Simpkins, B. S. & Owrutsky, J. C. Ultrafast transmission modulation and recovery via vibrational strong coupling. *J Phys Chem A* **122**, 965–971 (2018).
- [17] del Pino, J., Feist, J. & Garcia-Vidal, F. J. Quantum theory of collective strong coupling of molecular vibrations with a microcavity mode. *New J Phys* **17**, 053040 (2015).
- [18] Daskalakis, K. S., Maier, S. A. & Kéna-Cohen, S. *Polariton Condensation in Organic Semiconductors*, 151–163 (Springer International Publishing, Cham, 2017).
- [19] Xiang, B. *et al.* Two-dimensional infrared spectroscopy of vibrational polaritons. *Proceedings of the National Academy of Sciences* **115**, 4845 (2018).
- [20] Erwin, J., Smotzer, M. & Coe, J. V. Effect of strongly coupled vibration-cavity polaritons on the bulk vibrational states within a wavelength-scale cavity. *J Phys Chem B* **123**, 1302–1306 (2019).
- [21] Marcus, R. A. Chemical and electrochemical electron-transfer theory. *Annu Rev Phys Chem* **15**, 155–196 (1964).
- [22] Levich, V. Present state of the theory of oxidation-reduction in solution (bulk and electrode reactions). *Advances in electrochemistry and electrochemical engineering* **4**, 249–371 (1966).
- [23] Jortner, J. Temperature dependent activation energy for electron transfer between biological molecules. *J Chem Phys* **64**, 4860–4867 (1975).
- [24] Wang, D., Ivanov, M. V., Mirzaei, S., Lindeman, S. V. & Rathore, R. An electron-transfer induced conformational transformation: from non-cofacial sofa to cofacial boat in cyclotetrameratrylene (cttv) and formation of charge transfer complexes. *Org Biomol Chem* **16**, 5712–5717 (2018).
- [25] Khopde, S. M. & Priyadarsini, K. I. Application of marcus theory of electron transfer for the reactions between hrp compound i and ii and 2,4-disubstituted phenols. *Biophysical Chemistry* **88**, 103–109 (2000).
- [26] Walls, D. F. & Milburn, G. J. *Quantum Optics* (Springer Berlin Heidelberg, 2008).
- [27] Herrera, F. & Spano, F. C. Cavity-controlled chemistry in molecular ensembles. *Phys Rev Lett* **116**, 238301 (2016).
- [28] Semenov, A. & Nitzan, A. Electron transfer in confined electromagnetic fields. *J. Chem. Phys.* **150**, 174122 (2019).
- [29] Herrera, F. & Spano, F. C. Dark vibronic polaritons and the spectroscopy of organic microcavities. *Phys Rev Lett* **118**, 223601 (2017).
- [30] Houdré, R., Stanley, R. P. & Ilegems, M. Vacuum-field rabi splitting in the presence of inhomogeneous broadening: Resolution of a homogeneous linewidth in an inhomogeneously broadened system. *Phys. Rev. A* **53**, 2711–2715 (1996).
- [31] Mazza, L., Fontanesi, L. & La Rocca, G. C. Organic-based microcavities with vibronic progressions: Photoluminescence. *Phys. Rev. B* **80**, 235314 (2009).
- [32] Manceau, J.-M., Biasiol, G., Tran, N. L., Carusotto, I. & Colombelli, R. Immunity of intersubband polaritons to inhomogeneous broadening. *Phys. Rev. B* **96**, 235301 (2017).
- [33] Strashko, A. & Keeling, J. Raman scattering with strongly coupled vibron-polaritons. *Phys Rev A* **94**, 023843 (2016).
- [34] Heller, E. J. *The Semiclassical Way to Dynamics and Spectroscopy* (Princeton University Press, 2018).
- [35] Sando, G. M., Spears, K. G., Hupp, J. T. & Ruhoff, P. T. Large electron transfer rate effects from the Duschinsky mixing of vibrations. *J Phys Chem A* **105**, 5317–5325 (2001).
- [36] Huh, J., Guerreschi, G. G., Peropadre, B., McClean, J. R. & Aspuru-Guzik, A. Boson sampling for molecular vibronic spectra. *Nat Photonics* **9**, 615 (2015).
- [37] Du, M. *et al.* Theory for polariton-assisted remote energy transfer. *Chem Sci* **9**, 6659–6669 (2018).
- [38] Long, J. P. & Simpkins, B. S. Coherent coupling between a molecular vibration and Fabry-Perot optical cavity to give hybridized states in the strong coupling limit. *ACS Photonics* **2**, 130–136 (2015).
- [39] Shalabney, A. *et al.* Coherent coupling of molecular resonators with a microcavity mode. *Nat Commun* **6**, 5981 (2015).
- [40] Casey, S. R. & Sparks, J. R. Vibrational strong coupling of organometallic complexes. *J Phys Chem C* **120**, 28138–28143 (2016).
- [41] Vergauwe, R. M. A. *et al.* Quantum strong coupling with protein vibrational modes. *J Phys Chem Lett* **7**, 4159–4164 (2016).
- [42] Chaudhuri, S. *et al.* Electron transfer assisted by vibronic coupling from multiple modes. *J Chem Theory Comput* **13**, 6000–6009 (2017).
- [43] Mirjani, F., Renaud, N., Gorczak, N. & Grozema, F. C. Theoretical investigation of singlet fission in molecular dimers: The role of charge transfer states and quantum interference. *J Phys Chem C* **118**, 14192–14199 (2014).
- [44] Marcus, R. & Sutin, N. Electron transfers in chemistry and biology. *Biochimica et Biophysica Acta (BBA) - Reviews on Bioenergetics* **811**, 265 – 322 (1985).
- [45] Nitzan, A. *Chemical Dynamics in Condensed Phases: Relaxation, Transfer and Reactions in Condensed Molecular Systems*. Oxford Graduate Texts (OUP Oxford, 2006).
- [46] Orgiu, E. *et al.* Conductivity in organic semiconductors hybridized with the vacuum field. *Nat Mater* **14**, 1123 (2015).
- [47] Hagenmüller, D., Schachenmayer, J., Schütz, S., Genes, C. & Pupillo, G. Cavity-enhanced transport of charge. *Phys Rev Lett* **119**, 223601 (2017).
- [48] Cheng, C.-Y. *et al.* Charged polaron polaritons in an organic semiconductor microcavity. *Phys Rev Lett* **120**, 017402 (2018).
- [49] Möhl, C. *et al.* Trion-polariton formation in single-walled carbon nanotube microcavities. *ACS Photonics* **5**, 2074–2080 (2018).
- [50] Galego, J., Climent, C., Garcia-Vidal, F. J. & Feist, J. Cavity Casimir-Polder forces and their effects in ground state chemical reactivity (2018). Preprint, posted February 11, 2019.
- [51] Gillespie, D. T. Stochastic simulation of chemical kinetics. *Annu Rev Phys Chem* **58**, 35–55 (2007).
- [52] Keeling, J. & Kirton, P. G. Orientational alignment in cavity quantum electrodynamics. *Phys. Rev. A* **97**, 053836 (2018).

Supporting Information for Resonant catalysis of chemical reactions with vibrational polaritons

Jorge A. Campos-Gonzalez-Angulo, Raphael F. Ribeiro, and Joel Yuen-Zhou*
Department of Chemistry and Biochemistry. University of California San Diego. La Jolla, California 92093, USA

S1. Relation between reactant and product harmonic oscillator operators

Let us consider the vibrational Hamiltonians for the single-molecule reactant and product electronic states (we omit label (*i*) for simplicity hereafter),

$$\hat{H}_R = \frac{\hat{p}^2}{2m} + \frac{m\omega_R^2 \hat{x}^2}{2} = \hbar\omega_R \left(\hat{a}_R^\dagger \hat{a}_R + \frac{1}{2} \right), \quad (\text{S1})$$

$$\hat{H}_P = \frac{\hat{p}^2}{2m} + \frac{m\omega_P^2 (\hat{x} - d_P)^2}{2} + \Delta E = \hbar\omega_P \left(\hat{a}_P^\dagger \hat{a}_P + \frac{1}{2} \right) + \Delta E, \quad (\text{S2})$$

where m is the reduced mass of the mode, ω_A is the frequency of the mode in each electronic state ($A = R, P$), d_P is the difference between nuclear equilibrium configurations, ΔE is the energy difference between the electronic states, and \hat{p} and \hat{x} are the momentum and position operators for the described mode; therefore, the harmonic oscillator potential energy surface for P is a displaced-distorted version of that for R . The creation and annihilation operators are defined in terms of position and momentum ($d_R = 0$),

$$\begin{aligned} \hat{a}_A^\dagger &= \sqrt{\frac{\omega_A m}{2\hbar}} (\hat{x} - d_A) - \frac{i\hat{p}}{\sqrt{2\hbar\omega_A m}}, \\ \hat{a}_A &= \sqrt{\frac{\omega_A m}{2\hbar}} (\hat{x} - d_A) + \frac{i\hat{p}}{\sqrt{2\hbar\omega_A m}}; \end{aligned} \quad (\text{S3})$$

conversely, the position-momentum representation is written in terms of the creation and annihilation operators as

$$\begin{aligned} \hat{x} - d_A &= \sqrt{\frac{\hbar}{2\omega_A m}} (\hat{a}_A^\dagger + \hat{a}_A), \\ \hat{p} &= \sqrt{\frac{\hbar\omega_A m}{2}} i (\hat{a}_A^\dagger - \hat{a}_A). \end{aligned} \quad (\text{S4})$$

Eq. (S4) implies

$$\begin{aligned} \frac{\hat{a}_R^\dagger + \hat{a}_R}{\sqrt{\omega_R}} &= \frac{\hat{a}_P^\dagger + \hat{a}_P + \tilde{d}_P}{\sqrt{\omega_P}}, \\ \sqrt{\omega_R} (\hat{a}_R^\dagger - \hat{a}_R) &= \sqrt{\omega_P} (\hat{a}_P^\dagger - \hat{a}_P), \end{aligned} \quad (\text{S5})$$

where $\tilde{d}_P = \sqrt{2m/\hbar} d_P$; therefore, the reactant operators are written in terms of product ones as

$$\begin{aligned} \hat{a}_R^\dagger &= \frac{1}{2} \left(\sqrt{\frac{\omega_R}{\omega_P}} + \sqrt{\frac{\omega_P}{\omega_R}} \right) \hat{a}_P^\dagger + \frac{1}{2} \left(\sqrt{\frac{\omega_R}{\omega_P}} - \sqrt{\frac{\omega_P}{\omega_R}} \right) \hat{a}_P + \sqrt{\frac{\omega_R}{\omega_P}} \frac{\tilde{d}_P}{2}, \\ \hat{a}_R &= \frac{1}{2} \left(\sqrt{\frac{\omega_R}{\omega_P}} - \sqrt{\frac{\omega_P}{\omega_R}} \right) \hat{a}_P^\dagger + \frac{1}{2} \left(\sqrt{\frac{\omega_R}{\omega_P}} + \sqrt{\frac{\omega_P}{\omega_R}} \right) \hat{a}_P + \sqrt{\frac{\omega_R}{\omega_P}} \frac{\tilde{d}_P}{2}. \end{aligned} \quad (\text{S6})$$

These transformations can be written in terms of a squeezing and a displacement operator [1]:

$$\hat{S}_P(r) = \exp \left[\frac{r}{2} (\hat{a}_P^2 - \hat{a}_P^{\dagger 2}) \right], \quad (\text{S7})$$

$$\hat{D}_P(\alpha) = \exp \left[\alpha (\hat{a}_P^\dagger - \hat{a}_P) \right], \quad (\text{S8})$$

* joelyuen@ucsd.edu

with actions given by

$$\hat{S}_P^\dagger(r)\hat{a}_P^\dagger\hat{S}_P(r) = \hat{a}_P^\dagger \cosh r - \hat{a}_P \sinh r, \quad (\text{S9})$$

$$\hat{D}_P^\dagger(\alpha)\hat{a}_P\hat{D}_P(\alpha) = \hat{a}_P + \alpha. \quad (\text{S10})$$

Therefore,

$$\hat{a}_R^\dagger = \hat{D}_P^\dagger(\alpha)\hat{S}_P^\dagger(r)\hat{a}_P^\dagger\hat{S}_P(r)\hat{D}_P(\alpha) \quad (\text{S11})$$

$$\hat{a}_R = \hat{D}_P^\dagger(\alpha)\hat{S}_P^\dagger(r)\hat{a}_P\hat{S}_P(r)\hat{D}_P(\alpha),$$

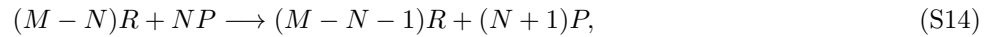
for

$$r = \ln \sqrt{\frac{\omega_R}{\omega_P}}, \quad (\text{S12})$$

$$\alpha = \tilde{d}_P. \quad (\text{S13})$$

S2. Initial and final many-body vibronic states

The rate to calculate corresponds to the stoichiometric process



where N is the number of molecules in the product electronic state P , and $M - N$ is the number of molecules in the reactant electronic state R , such that M is the total number of molecules in the reaction vessel. Assigning labels to each molecule, without loss of generality, the transformation of the $N + 1$ -th molecule can be written in the form

$$\sum_{i=N+1}^M R_i + \sum_{j=1}^N P_j \longrightarrow \sum_{i=N}^M R_i + \sum_{j=1}^{N+1} P_j, \quad (\text{S15})$$

which reduces to

$$R_{N+1} \longrightarrow P_{N+1}. \quad (\text{S16})$$

The charge transfer is ruled by the adiabatic coupling $\hat{J} = J_{RP} \sum_{i=1}^M (|R_i\rangle\langle P_i| + |P_i\rangle\langle R_i|)$; then, the matrix element that describes the process of our focus is

$$\langle M - N, N | \hat{J} | M - N - 1, N + 1 \rangle = J_{RP} \langle M - N, N | R_{N+1} \rangle \langle P_{N+1} | M - N - 1, N + 1 \rangle, \quad (\text{S17})$$

with many-body vibronic states given by

$$|X, Y\rangle = |P_1 P_2 \dots P_{Y-1} P_Y R_{Y+1} R_{Y+2} \dots R_{X+Y-1} R_{X+Y}\rangle \otimes |\Phi_X^Y\rangle, \quad (\text{S18})$$

where $|\Phi_X^Y\rangle$ is an eigenfunction of a vibrational Hamiltonian of the form

$$\begin{aligned} \hat{H}_{X,Y} &= \hat{H}_{\text{ph}} + \sum_{i=1}^Y \left(\hat{H}_P^{(i)} + \hat{\mathcal{V}}_{\text{int}}^{(i)} \right) + \sum_{j=Y+1}^{X+Y} \hat{H}_R^{(j)} \\ &= \hat{H}_{+(Y)} + \hat{H}_{-(Y)} + \sum_{k=1}^{Y-1} \hat{H}_{D(Y)}^{(k)} + \sum_{i=1}^Y \hat{H}_S(\hat{\mathbf{q}}_S^{(i)}) + Y\Delta E + \sum_{j=Y+1}^{X+Y} \hat{H}_R^{(j)}. \end{aligned} \quad (\text{S19})$$

In Eq. (S19), we have used the notation introduced in Eq. (2), and $\hat{H}_{\pm(Y)} = \hbar\omega_{\pm} \left(\hat{a}_{\pm(Y)}^\dagger \hat{a}_{\pm(Y)} + \frac{1}{2} \right)$ and $\hat{H}_{D(Y)}^{(k)} = \hbar\omega_P \left(\hat{a}_{D(Y)}^{\dagger(k)} \hat{a}_{D(Y)}^{(k)} + \frac{1}{2} \right)$ are the Hamiltonians of the upper/lower and k -th dark modes, respectively, all with creation and annihilation operators as defined in Eq. (3). Therefore, the matrix element corresponding to the transition becomes

$$\langle M - N, N | \hat{J} | M - N - 1, N + 1 \rangle = J_{RP} \langle \Phi_{M-N}^N | \Phi_{M-N-1}^{N+1} \rangle. \quad (\text{S20})$$

S3. Derivation of tridimensional Franck-Condon factor in Eq. (12)

The non-vanishing overlaps between the vibrational ground state of the reactants and an arbitrary vibrational excitation with quantum numbers $\{v_+, v_-, v_D\}$ on the products can be written in terms of creation operators as

$$\langle 0_0 0_{B(N-1)} 0'_N | v_+ v_- v_D \rangle = \langle 0_0 0_{B(N-1)} 0'_N | \frac{(\hat{a}_{+}^\dagger)^{v_+}}{\sqrt{v_+!}} \frac{(\hat{a}_{-}^\dagger)^{v_-}}{\sqrt{v_-!}} \frac{(\hat{a}_D^{(N-1)\dagger})^{v_D}}{\sqrt{v_D!}} | 0_{+(N)} 0_{-(N)} 0_D^{(N-1)} \rangle. \quad (\text{S21})$$

These operators acting in the *UP* and *LP* can be written as linear combinations of the operators acting on the electromagnetic mode and the bright mode [Eq. (3)], i.e.,

$$\begin{aligned} \langle 0_0 0_{B(N-1)} 0'_N | v_+ v_- v_D \rangle &= \langle 0_0 0_{B(N-1)} 0'_N | \frac{(\hat{a}_0^\dagger \cos \theta - \hat{a}_{B(N)}^\dagger \sin \theta)^{v_+}}{\sqrt{v_+!}} \frac{(\hat{a}_0^\dagger \sin \theta + \hat{a}_{B(N)}^\dagger \cos \theta)^{v_-}}{\sqrt{v_-!}} \\ &\quad \times \frac{(\hat{a}_D^{(N-1)\dagger})^{v_D}}{\sqrt{v_D!}} | 0_0 0_{B(N)} 0_D^{(N-1)} \rangle \end{aligned} \quad (\text{S22})$$

The binomial theorem yields

$$\begin{aligned} \langle 0_0 0_{B(N-1)} 0'_N | v_+ v_- v_D \rangle &= \sum_{m=0}^{v_+} \sum_{n=0}^{v_-} \binom{v_+}{m} \binom{v_-}{n} \langle 0_0 0_{B(N-1)} 0'_N | \frac{(\hat{a}_0^\dagger \cos \theta)^m (-\hat{a}_{B(N)}^\dagger \sin \theta)^{v_+ - m}}{\sqrt{v_+!}} \\ &\quad \times \frac{(\hat{a}_0^\dagger \sin \theta)^n (\hat{a}_{B(N)}^\dagger \cos \theta)^{v_- - n} (\hat{a}_D^{(N-1)\dagger})^{v_D}}{\sqrt{v_-!} \sqrt{v_D!}} | 0_0 0_{B(N)} 0_D^{(N-1)} \rangle. \end{aligned} \quad (\text{S23})$$

Since $[\hat{a}_0, \hat{a}_{B(N)}] = 0$, the only non-vanishing terms are those with $m = n = 0$, otherwise the overlap in the photonic mode would be between non-displaced states with different excitations; therefore,

$$\langle 0_0 0_{B(N-1)} 0'_N | v_+ v_- v_D \rangle = \langle 0_{B(N-1)} 0'_N | \frac{(-\hat{a}_{B(N)}^\dagger \cos \theta)^{v_+}}{\sqrt{v_+!}} \frac{(\hat{a}_{B(N)}^\dagger \sin \theta)^{v_-}}{\sqrt{v_-!}} \frac{(\hat{a}_D^{(N-1)\dagger})^{v_D}}{\sqrt{v_D!}} | 0_{B(N)} 0_D^{(N-1)} \rangle. \quad (\text{S24})$$

Moreover, the creation operators acting on the bright and dark modes can be expressed as linear combinations of operators acting on the N -th molecule and the bright mode that excludes it [Eq. (6)], i.e.,

$$\begin{aligned} \langle 0_0 0_{B(N-1)} 0'_N | v_+ v_- v_D \rangle &= \frac{(-\cos \theta)^{v_+} (\sin \theta)^{v_-}}{\sqrt{v_+! v_-! v_D!}} \langle 0_{B(N-1)} 0'_N | \left(\hat{a}_{B(N-1)}^\dagger \sqrt{\frac{N-1}{N}} + \hat{a}_N^\dagger \sqrt{\frac{1}{N}} \right)^{v_+} \\ &\quad \times \left(\hat{a}_{B(N-1)}^\dagger \sqrt{\frac{N-1}{N}} + \hat{a}_N^\dagger \sqrt{\frac{1}{N}} \right)^{v_-} \left(\hat{a}_{B(N-1)}^\dagger \sqrt{\frac{1}{N}} - \hat{a}_N^\dagger \sqrt{\frac{N-1}{N}} \right)^{v_D} | 0_{B(N-1)} 0_N \rangle. \end{aligned} \quad (\text{S25})$$

By expanding the binomials as before, and discarding the terms that excite the $B(N-1)$ mode, we arrive at

$$\begin{aligned} \langle 0_0 0_{B(N-1)} 0'_N | v_+ v_- v_D \rangle &= \frac{(-\cos \theta)^{v_+} (\sin \theta)^{v_-}}{\sqrt{v_+! v_-! v_D!}} \langle 0'_N | \left(-\hat{a}_N^\dagger \sqrt{\frac{1}{N}} \right)^{v_+} \left(\hat{a}_N^\dagger \sqrt{\frac{1}{N}} \right)^{v_-} \left(-\hat{a}_N^\dagger \sqrt{\frac{N-1}{N}} \right)^{v_D} | 0_N \rangle \\ &= \frac{1}{\sqrt{v_+! v_-! v_D!}} \left(-\frac{\cos \theta}{\sqrt{N}} \right)^{v_+} \left(\frac{\sin \theta}{\sqrt{N}} \right)^{v_-} \left(-\sqrt{\frac{N-1}{N}} \right)^{v_D} \langle 0'_N | (\hat{a}_N^\dagger)^{v_+ + v_- + v_D} | 0_N \rangle. \end{aligned} \quad (\text{S26})$$

Acting the creation operator on the N -th mode allows us to write

$$\langle 0_0 0_{B(N-1)} 0'_N | v_+ v_- v_D \rangle = \sqrt{\frac{(v_+ + v_- + v_D)!}{v_+! v_-! v_D!}} \left(-\frac{\cos \theta}{\sqrt{N}} \right)^{v_+} \left(\frac{\sin \theta}{\sqrt{N}} \right)^{v_-} \left(-\sqrt{\frac{N-1}{N}} \right)^{v_D} \langle 0'_N | (v_+ + v_- + v_D)_N \rangle. \quad (\text{S27})$$

Therefore, the square of the Franck-Condon factor in Eq. (S21) is

$$|\langle 0_0 0_{B(N-1)} 0'_N | v_+ v_- v_D \rangle|^2 = \binom{v_+ + v_- + v_D}{v_+, v_-, v_D} \left(\frac{\cos^2 \theta}{N} \right)^{v_+} \left(\frac{\sin^2 \theta}{N} \right)^{v_-} \left(\frac{N-1}{N} \right)^{v_D} |\langle 0'_N | (v_+ + v_- + v_D)_N \rangle|^2. \quad (\text{S28})$$

S4. Integrated Rate Law

Chemical Master Equation

The chemical master equation for the reaction in Eq. (7) is given by

$$\frac{\partial}{\partial t} \Pr(N_R, t | M, 0) = a(N_R + 1) \Pr(N_R + 1, t | M, 0) - a(N_R) \Pr(N_R, t | M, 0), \quad (\text{S29})$$

where $\Pr(n, t | m, 0)$ is the conditional probability to observe n molecules of the donor at time t given that there were m at $t = 0$, and $a(n) = nk_{R \rightarrow P}^{VSC}(n)$ is the propensity function [2]. Since $\Pr(M + 1, t | M, 0) \equiv 0$, this equation can be solved exactly by successively plugging $N_R = M, M - 1, \dots, 0$, yielding

$$\Pr(M - n, t | M, 0) = (-1)^n \prod_{i=0}^{n-1} a(M - i) \sum_{j=0}^n \frac{e^{-a(M-j)t}}{\prod_{\ell=0}^n [a(M - j) - a(M - \ell) + \delta_{j\ell}]}. \quad (\text{S30})$$

This probability density function can be used to determine the average number of donor molecules at a given time:

$$\langle N_R(t) \rangle \doteq \sum_{n=0}^M (M - n) \Pr(M - n, t | M, 0). \quad (\text{S31})$$

Taking the time derivative of this average yields Eq. (18).

However, for the number of molecules considered, $M = 10^7$, this calculation becomes intractable; therefore, we resort to the strategy described in the Materials and Methods section of the main manuscript and corroborate its validity with the stochastic simulation algorithm [2].

Stochastic Simulation Algorithm (SSA)

For the decomposition reaction in Eq. (18), we can define

$$p(\tau | M - n, t) = a(M - n) \exp(-a(M - n)\tau), \quad (\text{S32})$$

as the conditioned probability density function for the time of the next reaction (τ) given that the number of donor molecules left is $M - n$ at t . This function enables the construction of an exact numerical realization of the reaction with the following algorithm:

1. Initialize the system at $N_R(0) = M$.
2. With the system in state $N_R(t) = M - n(t)$, evaluate $a(N_R)$.
3. Generate a value for $\tau = -\ln(r)/a(N_R)$, where r is a uniformly distributed random number.
4. Perform the next reaction by making $N_R(t + \tau) = N_R(t) - 1$.
5. Register $N_R(t)$ as needed. Return to 2 or else end the simulation.

In Table S1, we show the correlation (r^2) between the reaction times calculated according to the mean-field finite difference approach described in the manuscript and the reaction times corresponding to the same step in the reaction with populations obtained from the mean of 100 trajectories computed with the SSA algorithm. Since these correlations are very close to the unity, we conclude that the compared methods are numerically equivalent [3]. These observations are consistent with a recent study that shows that mean-field theories provide good descriptions for polaritonic systems involving a large number of molecules [4].

[1] D. F. Walls and G. J. Milburn, *Quantum Optics* (Springer Berlin Heidelberg, 2008).

[2] D. T. Gillespie, *Annu Rev Phys Chem* **58**, 35 (2007).

[3] D. T. Gillespie, *J Phys Chem B* **113**, 1640 (2009).

[4] J. Keeling and P. G. Kirton, *Phys. Rev. A* **97**, 053836 (2018).

[5] A. Strashko and J. Keeling, *Phys Rev A* **94**, 023843 (2016).

TABLE S1.

Ω	Δ/ω_P	r^2
0	-	0.9970
	-0.02	0.9965
≥ 0	0	0.9982
	0.02	0.9973
	0.04	0.9970
	0.06	0.9969

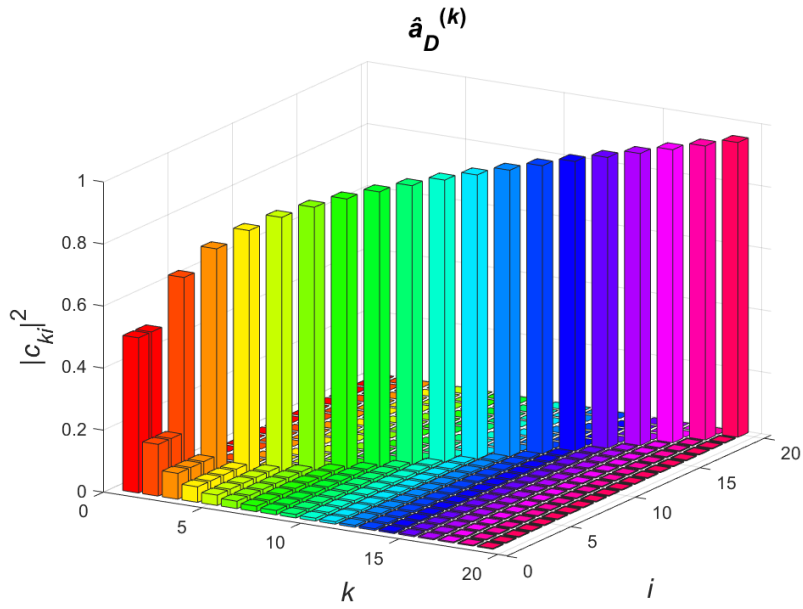


FIG. S1. Probability coefficients for each molecular mode in the quasi-localized basis of dark modes defined in Eq. (6). As the dark mode index, k , increases, it becomes more localized in the k -th molecule, leaving a long tail behind it [5].

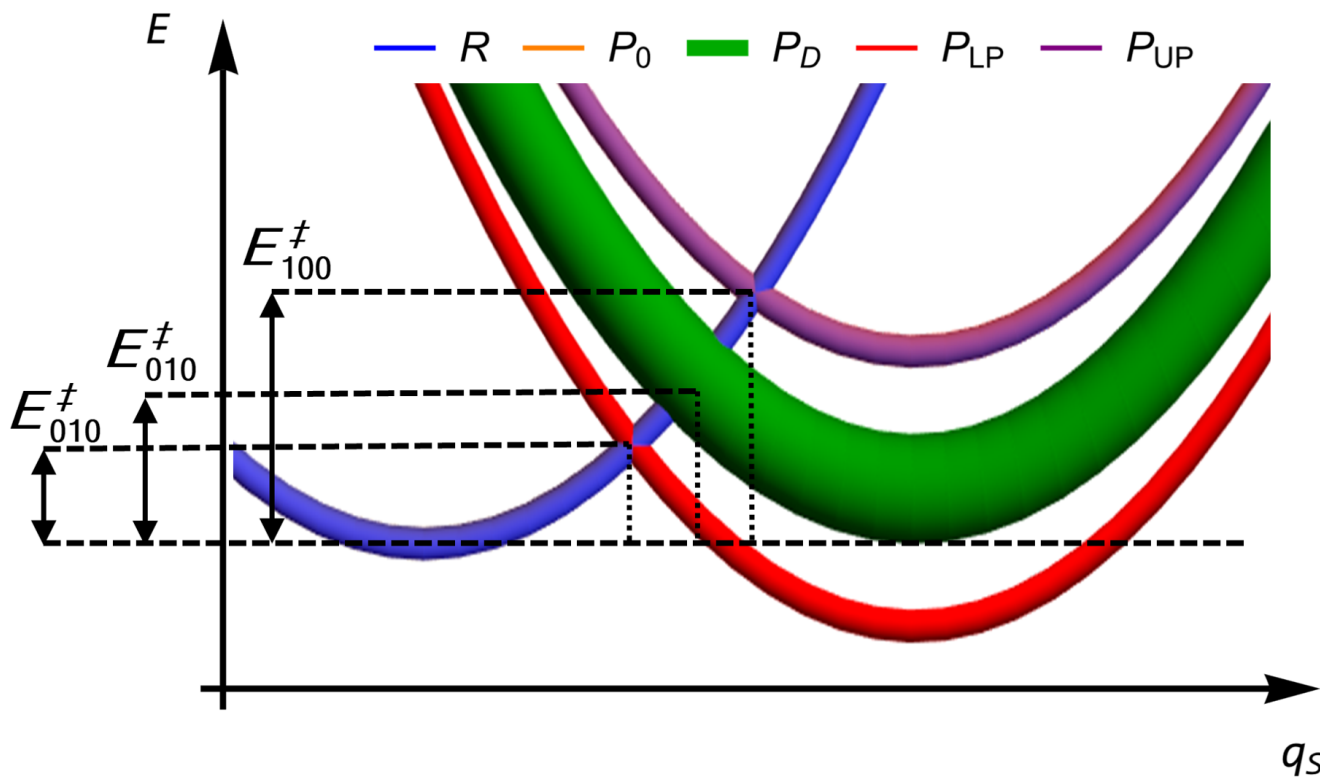


FIG. S2. Amplification of Fig. 3, showing a situation where a polariton channel dominates the kinetics of a reaction starting at reactant R . The channel involving a vibrational excitation in the lower polariton of the product (P_{LP}) features a small enough activation barrier E_{001}^\ddagger that can effectively compete against the many channels ending with a vibrational excitation in any of the dark modes, P_D , which feature corresponding activation energies E_{001}^\ddagger . These two activation energies are much smaller than E_{000}^\ddagger , the one associated with the channel leading to the global ground state of the products, P_0 (not shown in this amplified figure).